processes

MDPI

Article

Experimental Study on the Efficiency of Fracturing Integrated with Flooding by Slickwater in Tight Sandstone Reservoirs

Pingtian Fan [1,2], Yuetian Liu [1,*], Ziyu Lin [1,*], Haojing Guo [1] and Ping Li [2]

[1] State Key Laboratory of Petroleum Resources and Prospecting, China University of Petroleum (Beijing), Beijing 102249, China
[2] Nanniwan Oil Production Plant, Yanchang Oilfield Co., Ltd., Yan'an 716000, China
* Correspondence: lyt51@163.com (Y.L.); 2021310138@student.cup.edu.cn (Z.L.)

Abstract: Tight reservoirs, with their nanoscale pore structures and limited permeability, present significant challenges for oil recovery. Composite fracturing fluids that combine both fracturing and oil recovery capabilities show great potential to address these challenges. This study investigates the performance of a slickwater-based fracturing fluid, combined with a high-efficiency biological oil displacement agent (HE-BIO), which offers both production enhancement and environmental compatibility. Key experiments included tests on single-phase flow, core damage assessments, interfacial tension measurements, and oil recovery evaluations. The results showed that (1) the slickwater fracturing fluid effectively penetrates the rock matrix, enhancing oil recovery while minimizing environmental impact; (2) it causes substantially less damage to the reservoir compared to traditional guar gum fracturing fluid, especially in cores with little higher initial permeability; and that (3) oil recovery improves as HE-BIO concentration increases from 0.5% to 2.5%, with 2.0% as the optimal concentration for maximizing recovery rates. These findings provide a foundation for optimizing fracturing oil displacement fluids in tight sandstone reservoirs, highlighting the potential of the integrated fracturing fluid to enhance sustainable oil recovery.

Keywords: Ordos Basin; tight sandstone reservoir; integrated fracturing oil displacement; percolation characteristics; slickwater; oil recovery

Citation: Fan, P.; Liu, Y.; Lin, Z.; Guo, H.; Li, P. Experimental Study on the Efficiency of Fracturing Integrated with Flooding by Slickwater in Tight Sandstone Reservoirs. *Processes* **2024**, *12*, 2529. https://doi.org/10.3390/pr12112529

Academic Editor: Youguo Yan

Received: 10 October 2024
Revised: 1 November 2024
Accepted: 11 November 2024
Published: 13 November 2024

1. Introduction

China has vast tight reservoirs, with geological recoverable resources estimated at approximately 178.20 billion tons, while the technically recoverable portion stands around 17.65 billion tons [1]. These tight reservoirs are characterized by nanoscale pores, large specific surface areas, and pronounced micro-scale heterogeneity [2]. Such features contribute to significant interface effects between the reservoir fluids and rocks, which, in turn, severely limit fluid mobility, reducing both the production potential of individual wells and the overall recovery rates of oil fields [3,4].

To improve oil recovery in tight reservoirs, volume fracturing has become the dominant method both domestically and internationally [5,6]. This technique creates a fracture network in the reservoir matrix, facilitating a three-dimensional transformation of the reservoir [7]. However, a critical challenge remains in selecting an effective fracturing fluid, which plays a key role in creating and maintaining fractures [8,9]. In tight reservoirs, high-viscosity fluids are generally unnecessary due to their potential for fluid leakage, prompting a preference for water-based fracturing fluids, typically composed of low-viscosity guar gum and various types of slickwater [10]. Slickwater fluids mainly serve to transmit pressure and transport proppant during fracturing, with key components including drag reducers and other additives [11–14].

Despite these advances, traditional fracturing fluids such as guar gum have limitations, including high residue content that can damage the reservoir and reduce energy efficiency

during fluid recovery [15,16]. Furthermore, fracturing-induced interactions between the injected fluids and the reservoir rocks can lead to formation damage [17], including clay deflocculation, particle invasion, and water blockage, further decreasing hydrocarbon output [18].

Recent research has focused on integrating oil displacement capabilities into fracturing fluids, resulting in the development of multifunctional fluids that not only create fractures but also enhance oil recovery. Yan [19] explored a novel fracturing-production integral fluid based on cationic surfactants, which can improve the efficiency of oil extraction by modifying interfacial properties and enhancing fluid stability under reservoir conditions. Cong [20] investigated the mechanisms of fracture oil displacement agents specifically designed for ultra-low permeability reservoirs, indicating that these agents can significantly improve oil recovery by optimizing fluid flow and reducing residual oil saturation. Gao [21] developed a triple-responsive smart fluid that integrates oil expulsion capabilities with tight oil fracturing, showcasing versatility in response to varying reservoir conditions. Zhang [22] evaluated Janus-SiO_2 nanoparticles in viscoelastic surfactant fracturing fluids, demonstrating enhanced performance due to improved viscosity and stability, which facilitates better fracture propagation and oil displacement. Gao [23] employed nuclear magnetic resonance (NMR) to investigate the impact of various additives in fracturing fluids on oil recovery and showed that the cocamidopropyl hydroxysultaine (CHSB) additive effectively reduced the area of residual oil distribution, especially in small pores.

In this context, environmental concerns related to the use of chemical additives in fracturing fluids, especially regarding groundwater contamination and ecological impacts, remain significant. Biosurfactants, which are widely used in microbial enhanced oil recovery (MEOR), offer a promising alternative to chemical surfactants due to their environmental compatibility [24–27]. Althalb [28] assessed various bacterial strains for their ability to biotransform heavy crude oil and indicated that the Bacillus species achieved the highest oil recovery. Wu [29] and Han [30] analyzed the role of Bacillus species in enhanced oil recovery, emphasizing their effectiveness in biosurfactant production and oil emulsification across various reservoir conditions. Their experiments showed improved oil recovery rates of 5.66% and 19%, respectively. Although these properties make biosurfactants attractive for integrated fracturing oil displacement applications, there remains a need to investigate their effects under specific tight sandstone reservoirs.

Integrated fracturing fluid application faces challenges in tight reservoirs due to complex conditions, including variable pore structures and connectivity. Typically, fracturing fluids are flowed back and removed before production begins. However, the tight sandstone reservoirs in the Ordos Basin have low permeability (<2 mD) and low porosity (<10%) [31]. These reservoirs are primarily composed of argillaceous rocks and fine-grained sandstone. The pore throats in the fine-grained sandstone are small, typically ranging from 2 to 8 μm, with throat radii primarily between 20 and 150 nm. This multiscale distribution of micropores and nano-throats restricts fluid flow [32], making production heavily reliant on fracturing. Wells in this region initially exhibit high output, which declines rapidly, leading to low recovery efficiency [33]. Yaich [34] found that appropriate soaking times after fracturing can significantly enhance production by improving fluid flow and fracture propagation. Additionally, You [35] discussed the concept of achieving zero flowback rates in tight reservoirs, which can reduce environmental impacts and enhance resource efficiency. Currently, the fracturing oil displacement integrated process, with minimal flowback, has undergone pilot testing in well N199-2 of the Nanniwan oil field in the Ordos Basin. Following its production, oil output increased by 37.3% in the first year compared to the conventional volume fracturing of well N199-3 in the same group. However, despite these significant results, the process still faces limitations, and the efficiency of fracturing integrated with flooding by slickwater is still not fully understood. While research on integrated fracturing fluids has largely emphasized properties like drag reduction, proppant suspension, and flowback efficiency [36,37], further investigation into the microscale behavior of these fluids within tight reservoirs is needed to fully understand their impact on

oil recovery. Addressing these complexities is crucial for optimizing recovery in reservoirs such as those in the Ordos Basin and for advancing sustainable oil extraction practices.

Therefore, this study aims to investigate the micro-percolation characteristics of a novel fracturing oil displacement integrated slickwater fracturing fluid in tight sandstone reservoirs. Experiments included single-phase percolation tests, core damage assessments, interfacial tension measurements, and oil recovery rate evaluations. The findings will contribute to the optimization and broader application of integrated fracturing fluids in tight reservoirs, providing valuable insights for future field operations.

2. Experimental Methods and Samples

2.1. Experimental Materials

Figure 1 shows the following core samples. As shown in Figure 1a, cylindrical cores were selected for the single-phase percolation mechanism and the core damage experiment due to their ability to replicate natural reservoir conditions more accurately. The uniform shape promotes consistent fluid flow during testing and minimizes edge effects, making them ideal for studying the interactions between fracturing fluids and the rock matrix. In Figure 1b, cube cores were selected for the core flooding experiment due to their standardized dimensions and consistent properties. The uniform shape facilitates easier handling and reproducible results, making them ideal for comparative analysis.

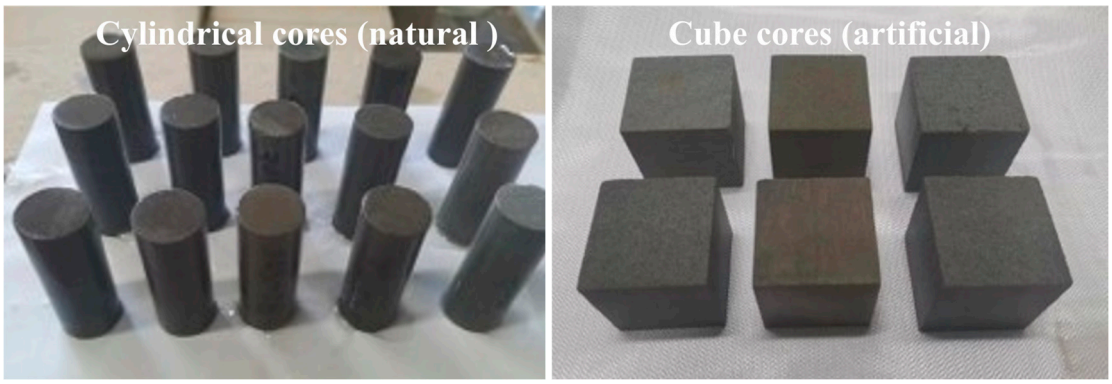

(**a**) (**b**)

Figure 1. (**a**) Natural cores from the tight reservoir of Chang 6 in the southwestern part of the Ordos Basin (Cores No. 1–16); (**b**) artificial cube cores (Cores No. 17–22).

The experimental cores used for the single-phase percolation mechanism experiment (Table 1) and the core damage experiment (Table 2) were tight sandstones from the Chang 6 formation in the southwestern part of the Ordos Basin. These cores exhibit varying porosity and permeability values, reflecting the reservoir conditions.

Table 1. Basic physical parameters of the natural cores used in the single-phase percolation mechanism experiment.

Core Number	Diameter (cm)	Length (cm)	Porosity (%)	Gas Permeability (mD)	Liquid Permeability (mD)	Average Liquid Permeabllity (mD)
1	2.5	6.42	8.80	0.1489	0.0409	0.0502 (higher permeabllity)
2	2.5	6.41	10.07	0.2039	0.0720	
3	2.5	6.42	8.67	0.1518	0.0378	
4	2.5	6.46	6.25	0.1156	0.0131	0.0127 (lower permeabllity)
5	2.5	6.46	5.94	0.1018	0.0108	
6	2.5	6.42	6.34	0.1220	0.0143	

Table 2. Basic physical parameters of the natural cores used in the core damage experiment.

Core Number	Diameter (cm)	Length (cm)	Porosity (%)	Gas Permeability (mD)	Liquid Permeability (mD)	Average Liquid Permeabllity (mD)
7	2.5	6.45	7.51	0.0708	0.0060	0.0119
8	2.5.	6.42	7.54	0.1011	0.0107	
9	2.5	6.44	8.77	0.1189	0.0137	
10	2.5	6.41	9.45	0.1005	0.0106	
11	2.5	6.51	9.61	0.1540	0.0257	
12	2.5	6.42	8.17	0.0789	0.0073	
13	2.5	6.42	8.80	0.0794	0.0073	
14	2.5	6.45	9.07	0.1005	0.0106	
15	2.5	6.42	4.71	0.0821	0.0078	
16	2.5	6.44	3.76	0.1418	0.0193	

In contrast, the experimental cores used for the core flooding experiment are artificial cube cores, which possess nearly uniform porosity and permeability (Table 3). These artificial cores represent the optimal physical properties among the reservoir condition, ensuring consistency in evaluating oil recovery.

Table 3. Basic physical parameters of artificial cube cores used in the core flooding experiment.

Core Number	Edge Length (cm)	Porosity (%)	Permeability (mD)	Average Permeabllity (mD)
17	5	11.37	0.1650	0.1661
18	5	11.04	0.1619	
19	5	11.36	0.1650	
20	5	11.98	0.1723	
21	5	11.52	0.1667	
22	5	11.44	0.1656	

Guar gum, clay stabilizer, drainage aid, bactericide, initiator, organic boron cross-linking agent, gel breaker, borax, drag-reducing agent, additive, oil displacement agent, crude oil, formation water, and other reagents were all provided by the Nanniwan Oil Production Plant. Formation water was water produced from the mine, with an average salinity of 35,273.99 mg/L (Table 4).

Table 4. Ionic Composition of the formation water in the experiment.

Na^+ (mg/L)	K^+ (mg/L)	Mg^{2+} (mg/L)	Ca^{2+}(mg/L)	Cl^- (mg/L)	CO_3^{2-} (mg/L)	Salinity (mg/L)
9018.16	87.29	70.39	4265.33	21,698.53	134.29	35,273.99

The slickwater fracturing fluid used in this study was formulated according to Shi et al. [38,39]. It consisted of 0.1% JHFR-2 drag reducer and 0.2% JHFD-2 multifunctional additive. This composition created a fracturing fluid with characteristics such as the following: it was an instant solution (within 30 s); it possessed nontoxicity; it provided environmental protection, low damage, drag reduction, and salt resistance; and it had anti-swelling properties and ultra-low interfacial tension, with a drag reduction rate of more than 75%. The prepared fluid was a colorless, transparent liquid with no precipitation, and had an average viscosity and molecular beam size of 1.6 mPa·s and 22 nm, respectively.

When microorganisms are cultured under specific conditions, amphiphilic compounds known as biosurfactants can be produced. These compounds integrate hydrophilic and hydrophobic group structures in the same molecule. Biosurfactants can be categorized into glycolipids, lipopeptides, phospholipids, fatty acid neutral lipids, and polymer complexes

combining polysaccharides and proteins. Lipopeptide surface-active oil displacement can enhance the oil-washing efficiency of water-driven reservoirs by reducing the interfacial tension between oil and water in oilfields [40,41]. The HE-BIO used is a metabolite of a strain of Bacillus velezensis with high lipopeptide production and is obtained from the formation of the oil field. The production process involved microbial fermentation technology, shaking bed incubation for 72 h at 36 °C and 180 r/min, centrifugation to remove the bacterium, pH adjustment of the upper layer of the clear liquid, and extraction after standing. The HE-BIO was obtained by separating and extracting the lower layer and removing the solvent.

The guar gum fracturing fluid used in this study comprised 0.3% guar gum, 0.5% clay stabilizer, 0.3% drainage aid, 0.1% bactericide, 0.1% initiator, 0.5% organic boron cross-linker, and 0.1% gel breaker. The viscosity of this fluid was 2.02 mPa·s.

The crude oil used in the experiments was sourced from the Chang 6 formation. Table 5 provides the physicochemical properties of the oil, including viscosity, density, total acid number (TAN), total base number (TBN), and SARA fractions (saturated hydrocarbons, aromatics, resins, and asphaltenes). Before testing, the samples were centrifuged to eliminate potential emulsions and solids.

Table 5. Parameters of the crude oil in the experiment.

Viscosity (mPa·s)	Density ($g \cdot cm^{-3}$)	TAN ($mgKOH \cdot g^{-1}$)	TBN ($mgKOH \cdot g^{-1}$)	Volume Fraction of Components			
				Saturated Hydrocarbons	Aromatics	Resin	Asphaltenes
formation water	9018.16	87.29	70.39	73.51%	21.53%	2.33%	2.63%

2.2. Single-Phase Percolation Mechanism Experiment

In this experiment, single-phase percolation tests were conducted on tight reservoir cores from the Ordos Basin to study the flow characteristics of formation water, slickwater, and guar gum fracturing fluids.

Figure 2 illustrates the experimental setup used for single-phase percolation testing. The setup consists of a fluid injection pump that regulates the flow of different fluids (formation water, slickwater, and guar gum fluid) through the core sample. Intermediate containers containing each fluid type are connected to the pump, allowing for controlled injection. Check valves prevent backflow and ensure that fluids flow in a unidirectional path. The core sample is placed in a core gripper, which is surrounded by a high-pressure confining jacket to simulate in situ reservoir pressures. Pressure gauges positioned before and after the core gripper monitor the pressure drop across the core. A back pressure regulator is located at the outlet to maintain consistent outlet pressure. Finally, production fluid is collected and analyzed to evaluate flow characteristics.

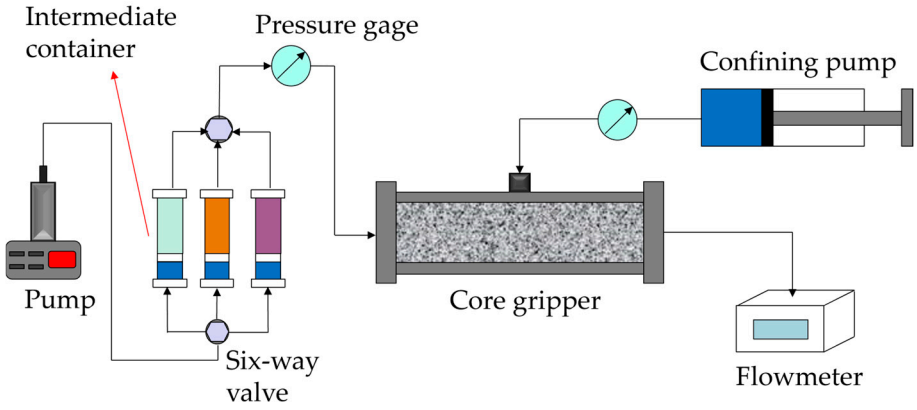

Figure 2. Flow chart of seepage characteristics experiment.

The experimental procedure involved the following steps:

(1) Cores No. 1–6 were dried in a vacuum oven at 120 °C for 3 days.
(2) Porosity and gas permeability were measured using nitrogen porosity and gas permeability tests.
(3) The dry cores were vacuum-saturated with formation water and pre-aged for 1 week.
(4) Saturated cores were placed in a core gripper and injected with formation water at a constant rate of 0.1 mL/min under a 30 MPa confining pressure to measure fluid permeability.
(5) The flow rate of formation water was varied, maintaining the 30 MPa confining pressure, and the stabilized differential pressure at each flow rate was recorded to plot the percolation curves.
(6) Slickwater and guar gum fracturing fluids were injected under the same conditions, and their differential pressures were recorded to generate the respective percolation curves. Since the core structure undergoes irreversible changes after being flooding by fracturing fluids, selected cores were reserved for specific fracturing fluid comparisons. Specifically, Cores No. 1, 2, 5, and 6 were used for slickwater testing, while Cores No. 3 and 6 were designated for guar gum fluid testing.

2.3. Core Damage Experiment

Tight oil reservoirs present significant challenges due to their poor physical properties and complex pore-permeability relationships. Hydraulic fracturing can cause additional damage to these reservoirs, making it crucial to address this issue during the development of tight oil fields. The slickwater fracturing fluid discussed in this study was designed to mitigate such damage.

The modification of the reservoir using the fracturing oil displacement integrated slickwater fracturing fluid involves two main processes: (1) the creation of hydraulic fractures through the injection of slickwater fracturing fluid, which enhances the permeability of the reservoir; (2) the fluid then enters the matrix through these fractures, where surfactants reduce interfacial tension and emulsify crude oil. This reduces capillary pressure and enhances oil mobility, resulting in more efficient oil displacement.

Figure 3 depicts the flow chart of the core damage experiment, which simulates the effect of fracturing fluid entering the reservoir matrix through fractures. In the experiment, core samples obtained from the Chang 6 formation of the Ordos Basin were used to simulate the matrix, aiming to achieve a realistic representation of reservoir conditions.

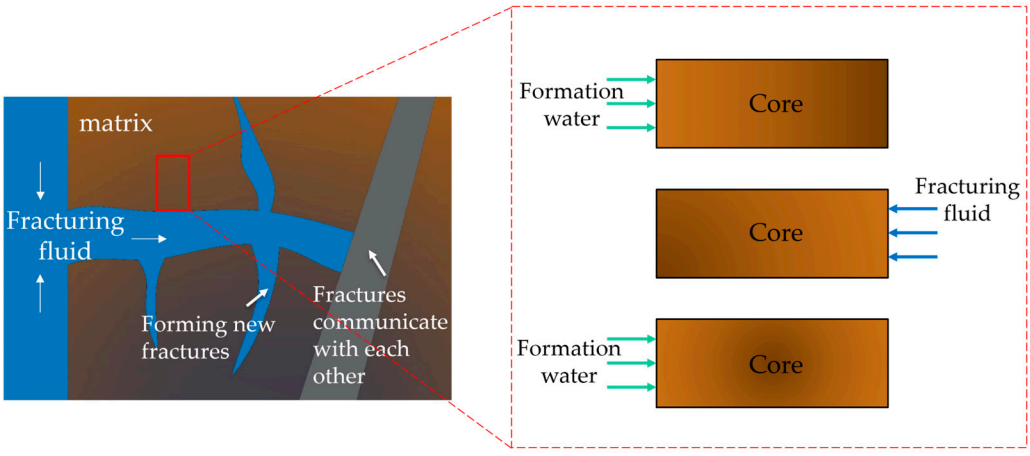

Figure 3. Flow chart of core damage experiment: green arrows indicate fluid entering the matrix, and blue arrows indicate fluid exiting the matrix.

We followed the Chinese performance evaluation method of water-based fracturing fluid (SY/T 5107-2016). The experimental apparatus is the same as that of the single-phase percolation mechanism experiment, and the experimental steps are as follows:

(1) We dried Cores No. 7–16 in a vacuum-drying oven at 120 °C for 3 days.

(2) We measured the porosity and permeability of each core. The permeability calculation follows Darcy's law:

$$K = \frac{Q\mu L}{A\Delta P} \quad (1)$$

where K is the permeability of the core, mD; Q is the flow rate of the fluid through the core, mL/min; μ is the fluid viscosity, mPa·s; L is the length of the core, cm; A is the cross-sectional area of the core, cm^2; and ΔP is the pressure drop across the core, MPa.

(3) Dry cores were vacuum saturated by immersion in formation water and pre-aged for 1 week. Then, permeability was measured with formation water.

(4) We introduced the slickwater fracturing fluid into the intermediate container and pressurized it with a pump to enable the fluid to enter the core from the inlet of the reverse end of the core gripper for 1 PV. The experimental apparatus was maintained at a temperature of 30 °C (formation temperature), and the injection pressure was set at 10 MPa (formation pressure), as per the relevant requirements in the evaluation standard.

(5) After injecting the fracturing fluid, we closed the valve at the end of the gripper to retain the fluid in the rock core for 2 h.

(6) We pumped formation water into the intermediate container, modeling the flowback process of the fracturing fluid in the field by reverse flooding.

(7) We measured the porosity and permeability of the cores after the reaction with the slickwater fracturing fluid. Permeability was calculated according to Darcy's law, and the damage percentage of the cores was determined as follows:

$$\eta_d = \frac{K_0 - K_d}{K_0} \times 100\% \quad (2)$$

where η_d is the permeability damage percentage, %; K_0 is the initial permeability before exposure, mD; K_d is the permeability after exposure to the slickwater fracturing fluid, mD.

(8) We replaced the core and repeated the experiment using the slickwater fracturing fluid or the guar gum fracturing fluid.

2.4. Interface Tension Measurement

In the study, HE-BIO was added to the slickwater fracturing fluid, which consisted of 0.1% JHFR-2 drag reducer and 0.2% JHFD-2 multifunctional additive, with concentration gradient settings of 0.5%, 1.0%, 1.5%, 2.0%, and 2.5%, respectively, as shown in Figure 4.

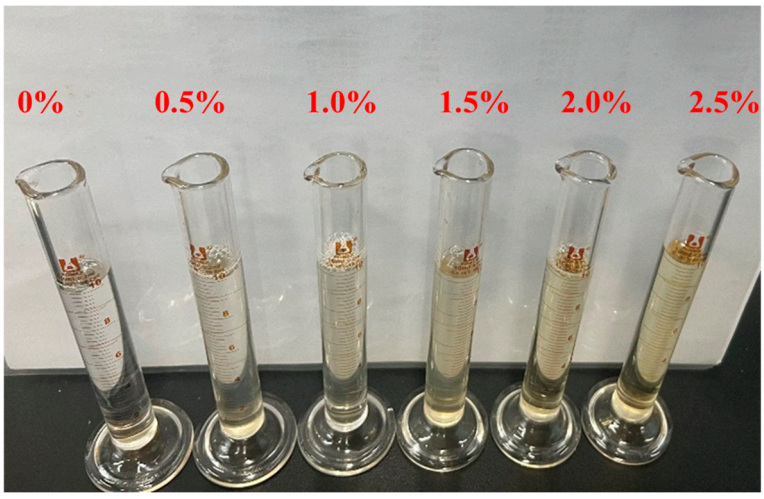

Figure 4. This figure shows 0.1% JHFR-2 and 0.2% JHFD-2 with different concentrations of HE-BIO.

The highest concentration of 2.5% was chosen to assess the upper limits of HE-BIO's effectiveness and to determine whether similar interfacial tension reduction and recovery rates could be achieved at lower concentrations. Typically, a concentration of 0.5% is used in field applications due to cost considerations, while testing at 2.5% enabled us to understand the full potential of HE-BIO in maximizing oil displacement efficiency.

The interfacial tension between crude oil and different fluids was measured using the pendant drop method and its oscillation function, as shown in Figure 5. A U-shaped needle was immersed in the formation water, and then the tip of the needle dripped crude oil at a rate of 15 µL/min. This process was captured by a CCD in real time to record the interfacial tension at the moment of droplet rupture. The temperature and pressure were maintained at 30 °C for all experiments.

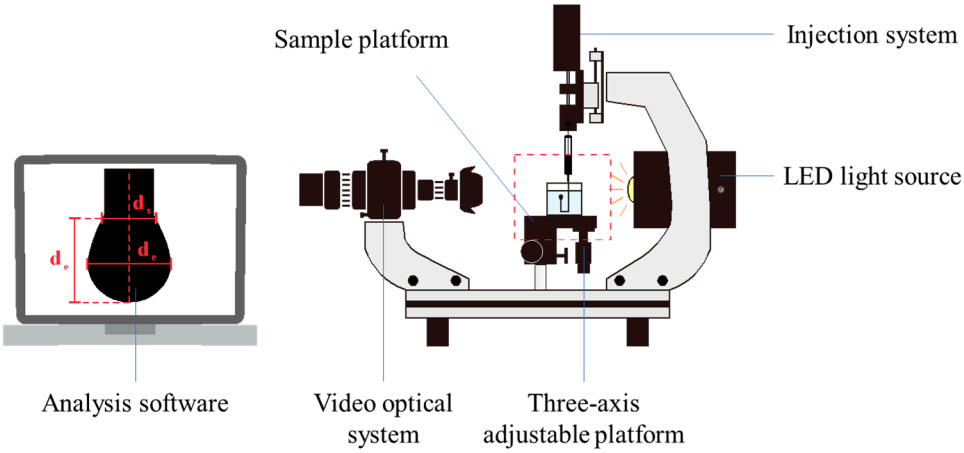

Figure 5. Interface tension measuring device.

The droplet dimensions (d_s and d_e) are displayed on a connected computer screen for precise measurement and calculation. The drop shape analysis allows for accurate determination of interfacial tension between fluids. Interfacial tension is calculated as follows:

$$\sigma = \frac{\Delta\rho g d_e^2}{H} \quad (3)$$

where σ is the interfacial tension, mN/m; $\Delta\rho$ is the density difference between two phases, g/cm^3; d_e is the equatorial diameter of the drop, cm; H is the shape parameter, which is related to the d_e and d_s and is dimensionless; and d_s is the diameter measured at a distance d_e from the top of the drop, cm.

2.5. Core Flooding Experiment

Cube rock Cores No. 17–22 were dried in a vacuum oven at 120 °C for three days until their weight stabilized. The cores were then vacuum-saturated with formation water and pre-aged for one week to ensure full saturation. Fluid permeability tests were conducted by placing the cores in a cube core gripper under 30 MPa confining pressure and injecting formation water at a constant rate of 0.1 mL/min. Crude oil was then injected at 10 MPa until water production stopped. Initial oil and bound water saturations were calculated, and the cores were aged for an additional week at 30 °C.

The displacement experiment, shown in Figure 6, used a precision injection pump (Teledyne ISCO 500×, Lincoln, NE, USA), an intermediate vessel, and a cube core gripper (Haian Oil Scientific Instrument Co., Ltd., Jiangsu, China). Displacement tests were conducted under 30 MPa confining pressure at 30 °C, with fluid injection at 0.1 mL/min. Oil and water production were monitored in real time using a high-precision oil–water separator and an electronic balance (Mettler XPR204S/AC, Mettler Toledo, Zurich, Switzerland). Initially, slickwater without HE-BIO was injected. Once the outlet pressure stabilized and

the water cut rate exceeded 98%, slickwater containing different HE-BIO concentrations was introduced until pressure stabilized and the water cut rate again reached 98%.

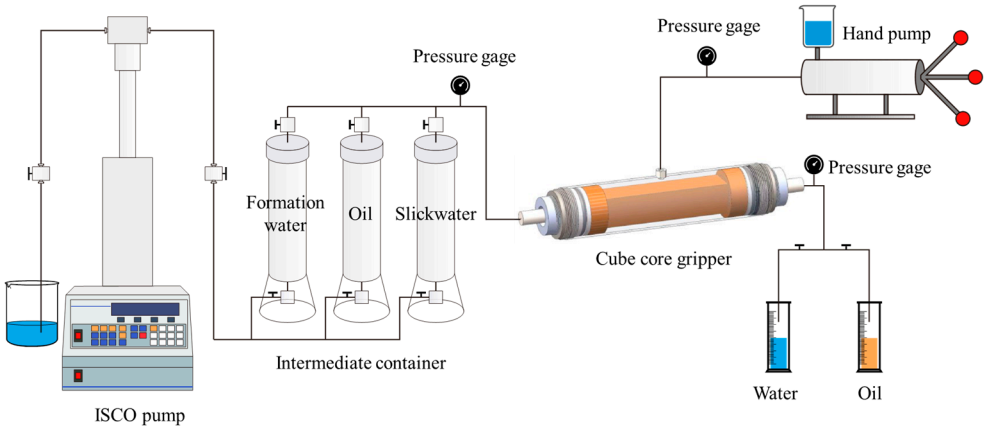

Figure 6. Displacement experiment analysis system.

The experimental procedures outlined above were carefully conducted to assess the fluid's performance under conditions representative of tight sandstone reservoirs. The results of these experiments are presented in the following section, showcasing key findings on fluid behavior, core damage, and recovery efficiency.

3. Results

3.1. Single-Phase Percolation Mechanism

Table 1 indicates an average permeability of 0.0502 mD for Cores No. 1–3 and 0.0127 mD for Cores No. 4–6, classifying them as tight reservoir cores. Figure 7 shows the single-phase percolation characteristic curves of formation water for the six cores, where the flow rate and pressure gradients are essentially a straight line for the higher permeability cores and for the lower permeability cores, which conforms to Darcy's law.

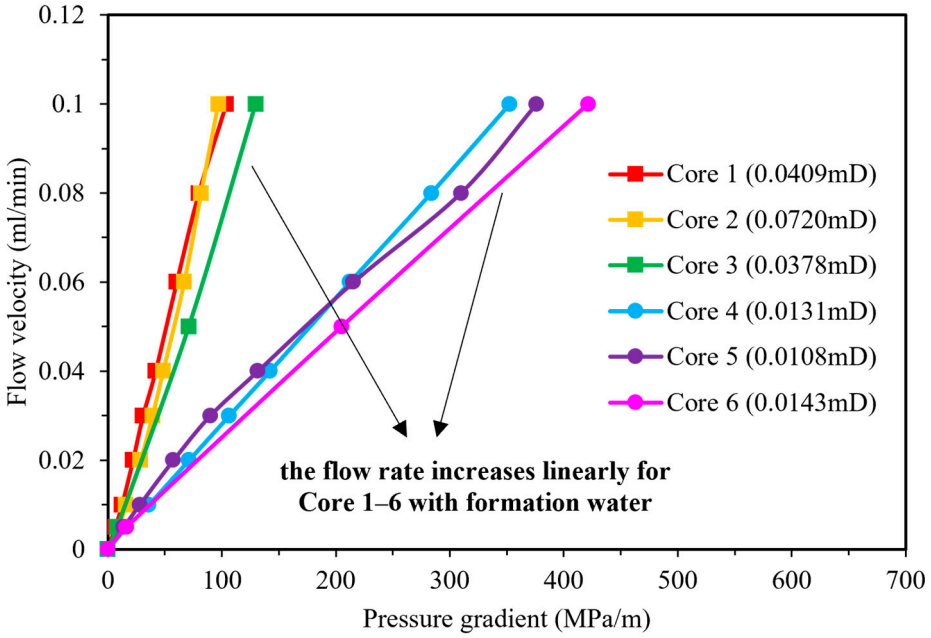

Figure 7. Percolation characteristic curves of formation water.

Figure 8 illustrates the single-phase percolation characteristic curves of the slickwater fracturing fluid in Cores 1, 2, 4, and 5. The higher permeability cores exhibit a linear

relationship, which is consistent with Darcy's law. Conversely, the single-phase percolation characteristic curves of the oil slick in the lower permeability cores display a downward curvature. This observation indicates that the nonlinear characteristics of the slickwater fracturing fluid percolation increase with decreasing permeability.

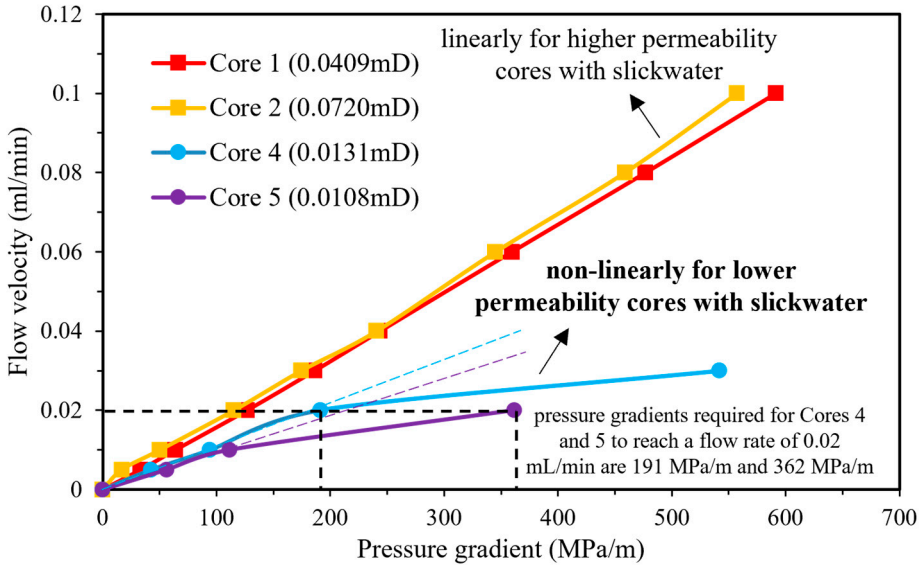

Figure 8. Percolation characteristic curves of the slickwater fracturing fluid (0.1% JHFR-2 + 0.2% JHFD-2).

Figure 9 illustrates the percolation characteristic curves of the guar gum fracturing fluid for Cores 3 and 6. The flow velocity and pressure gradient curves show a downward-bending nonlinearity for both the higher permeability cores and the lower permeability cores. This nonlinear behavior suggests that as the permeability of cores decreases, the guar gum fracturing fluid experiences an increasingly higher-pressure gradient that is even more pronounced than that of the slickwater.

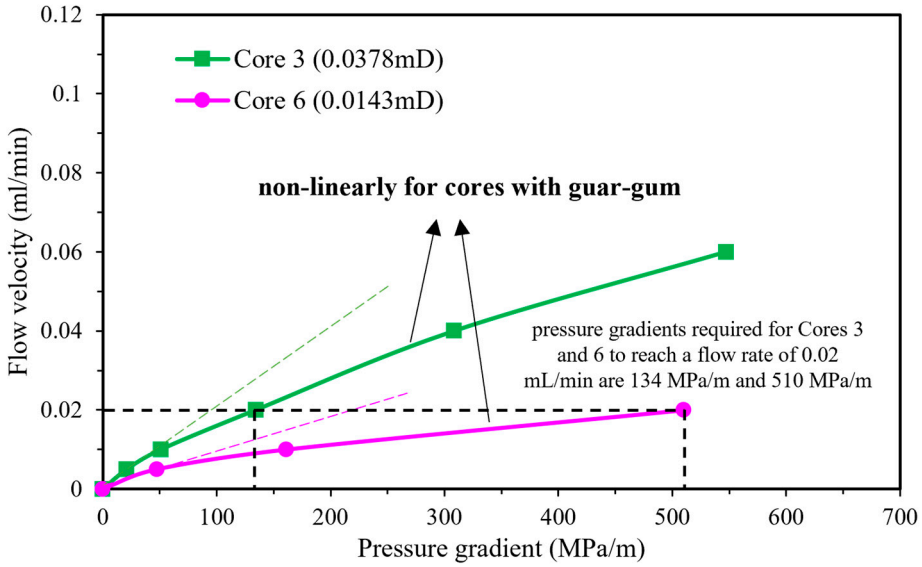

Figure 9. Percolation characteristic curves of the guar gum fracturing fluid.

3.2. Core Damage Caused by Fracturing Fluids

Cores No. 7–16 from Table 2, with an average permeability of 0.0119 mD, were utilized in the core damage experiment. The results, depicted in Table 6 and Figure 10, reveal

that the guar gum fracturing fluid caused an average damage percentage of 51.5% to the reservoir cores, with no clear correlation to the initial core permeability. In contrast, the slickwater fracturing fluid induced a significantly lower average damage percentage of 28.8%, falling below the 30% threshold specified in SY/T 6376-2008, "General Technical Conditions for Fracturing Fluid". This suggests that the slickwater fracturing fluid causes minimal reservoir damage during well shut-in after fracturing.

Table 6. Experimental results of core matrix permeability damage.

Core Number	Fracturing Fluid	Initial Permeability (mD)	Permeability After Damage (mD)	Damage Percentage (%)	Average Damage Percentage (%)
7	Slickwater fracturing fluid (0.1%JHFR-2 + 0.2%JHFD-2)	0.0060	0.0037	38.33	28.80
8		0.0107	0.0073	31.78	
9		0.0137	0.0106	24.90	
10		0.0106	0.0078	26.42	
11		0.0257	0.0193	22.63	
12	Guar gum fracturing fluid	0.0073	0.0035	52.05	51.49
13		0.0073	0.0036	50.68	
14		0.0106	0.0051	51.89	
15		0.0078	0.0037	52.56	
16		0.0193	0.0093	50.26	

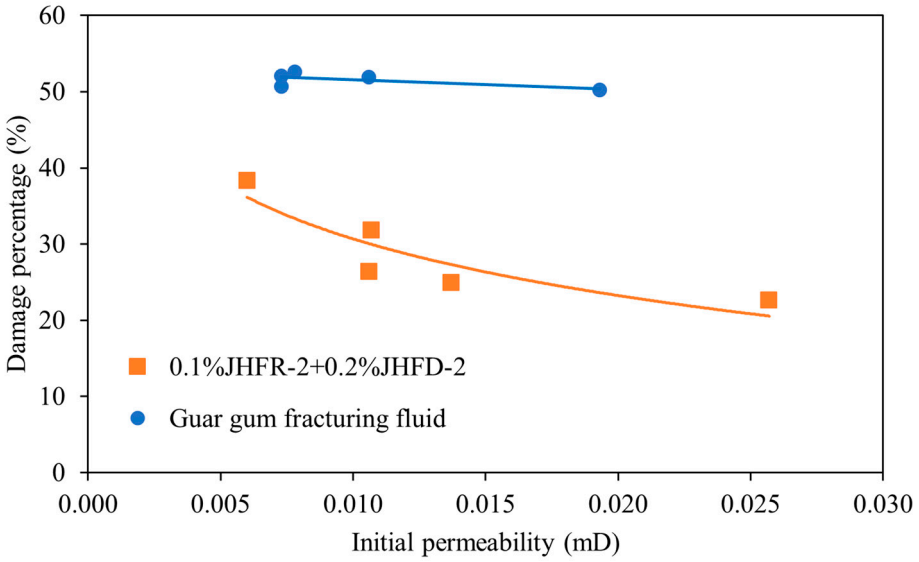

Figure 10. Relationship between the damage percentage of Cores No. 7–16 and initial permeability.

3.3. Interface Tension

Figures 11 and 12 depict the change in oil–water interfacial tension with different fluids.

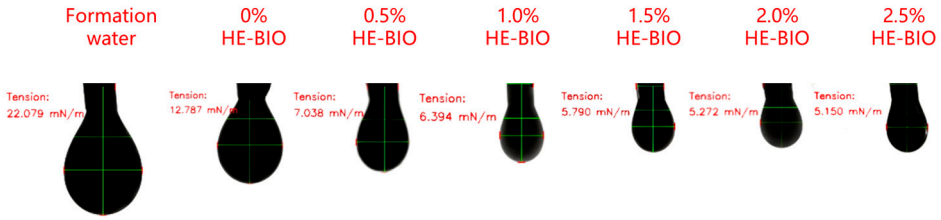

Figure 11. Oil–water interface tension in the fracturing oil displacement integrated slickwater fracturing fluid.

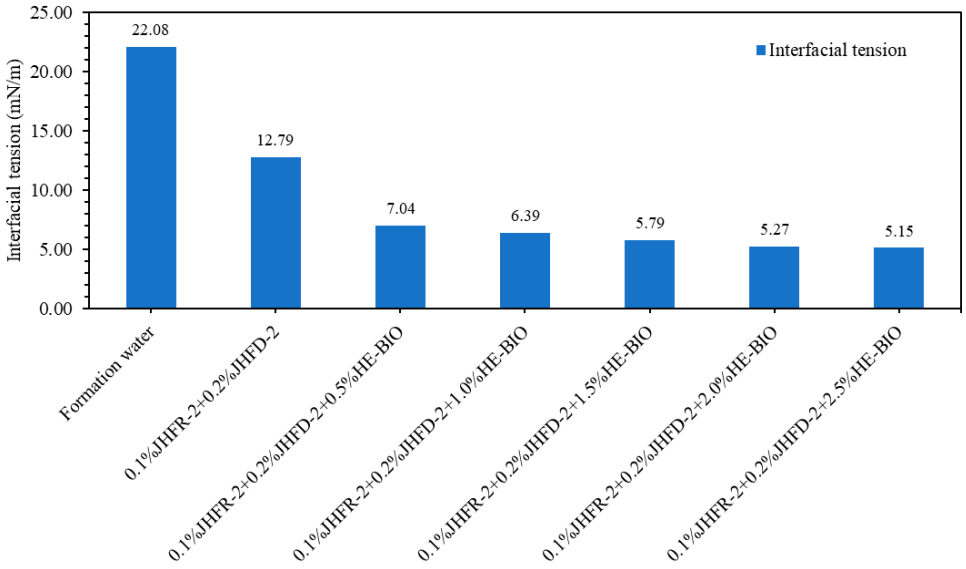

Figure 12. Oil–water interface tension changes in the fracturing oil displacement integrated slickwater fracturing fluid.

The result indicates that the interfacial tension between the formation water and oil was the highest at 22.079 mN/m. In comparison to formation water, the slickwater fracturing fluid significantly improved the interfacial tension between oil and water, with a value of 12.787 mN/m. The addition of HE-BIO to the slickwater fracturing fluid further reduced the oil–water interfacial tension, with the maximum reduction being 7.038 mN/m at a 0.5% concentration, and then the reduction became smaller.

3.4. Effect of Core Flooding

The fluids used to improve oil recovery rate in Cores No. 17–22 are outlined in Table 7, while the oil recovery rate with water flooding pore volume throughout the drive is shown in Figure 13.

Table 7. Parameters of the crude oil in the experiment.

Core Number	First Flooding Fluid	Oil Recovery Rate (%)	Second Flooding Fluid	Oil Recovery Rate (%)
17	Formation water	37.63	Formation water	39.21
18	Slickwater fracturing fluid (0.1%JHFR-2 + 0.2%JHFD-2)	41.04	0.1%JHFR-2 + 0.2%JHFD-2 + 0.5%HE-BIO	48.79
19		41.03	0.1%JHFR-2 + 0.2%JHFD-2 + 1.0%HE-BIO	50.76
20		40.99	0.1%JHFR-2 + 0.2%JHFD-2 + 1.5%HE-BIO	52.13
21		41.04	0.1%JHFR-2 + 0.2%JHFD-2 + 2.0%HE-BIO	53.21
22		41.02	0.1%JHFR-2 + 0.2%JHFD-2 + 2.5%HE-BIO	53.44

After flooding with slickwater fracturing fluid, the oil recovery rates for the three cores stabilized at 41.04%, 41.03%, and 40.99%. When switched to slickwater containing HE-BIO, recovery rates improved to 48.79%, 50.76%, 52.13%, 53.21%, and 53.44%. Figure 14 illustrates the relationship between the increase in viscosity and oil recovery rate as the HE-BIO concentration rises.

The results demonstrate several notable effects of the fracturing oil displacement fluid on tight cores. These findings provide the basis for a deeper analysis of the fluid's mechanisms and its potential implications for practical field applications, which are discussed in the following section.

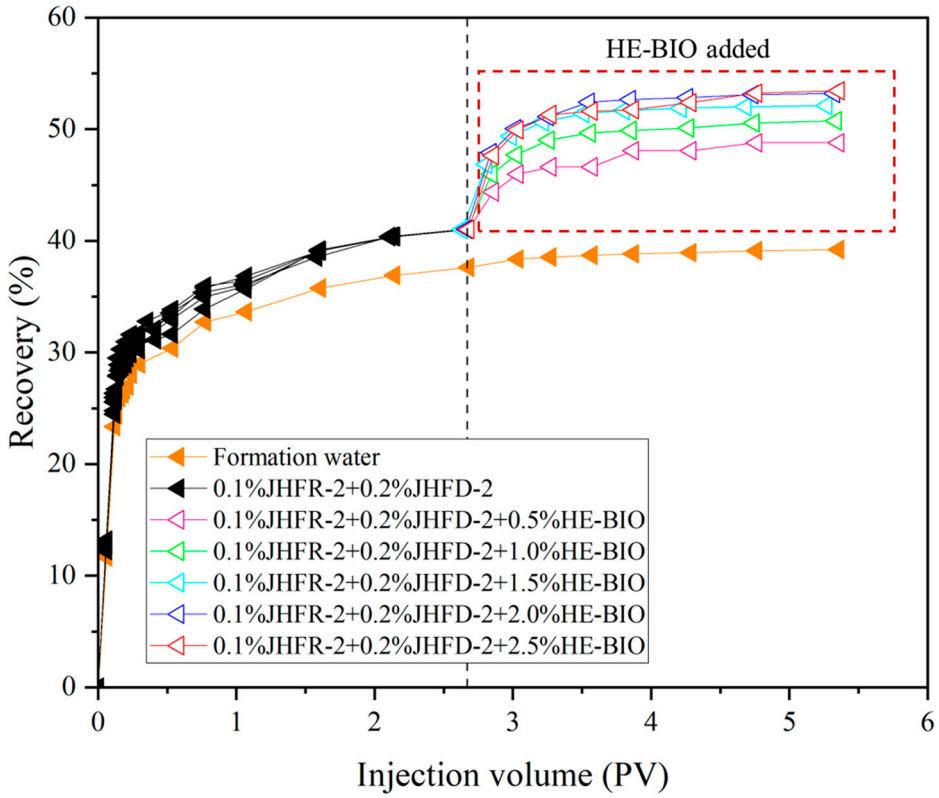

Figure 13. Oil recovery rate with pore volume.

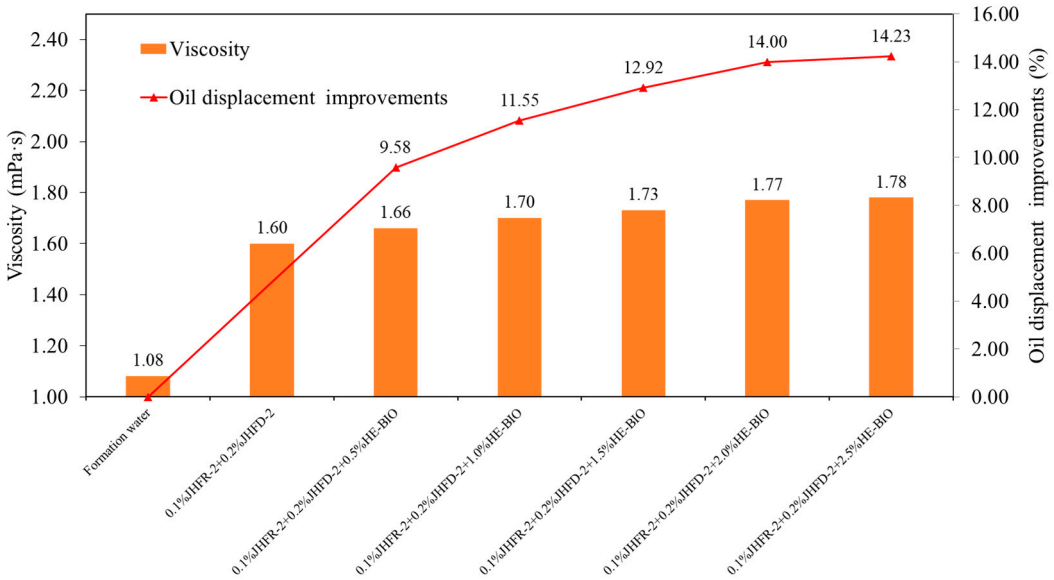

Figure 14. The viscosity and oil recovery rate values increase compared to formation water with the increasing concentration of HE-BIO.

4. Discussion

4.1. Core Damage Findings for Field Applications

Figure 15 illustrates the inlet ends of cores from the single-phase percolation mechanism experiment. Figure 15a shows Core 4, which was treated with the slickwater fracturing fluid and did not display any filter cake formation. In contrast, Figure 15b shows Core 4, which was treated with the guar gum fracturing fluid and exhibits a visible filter cake layer at the core entrance.

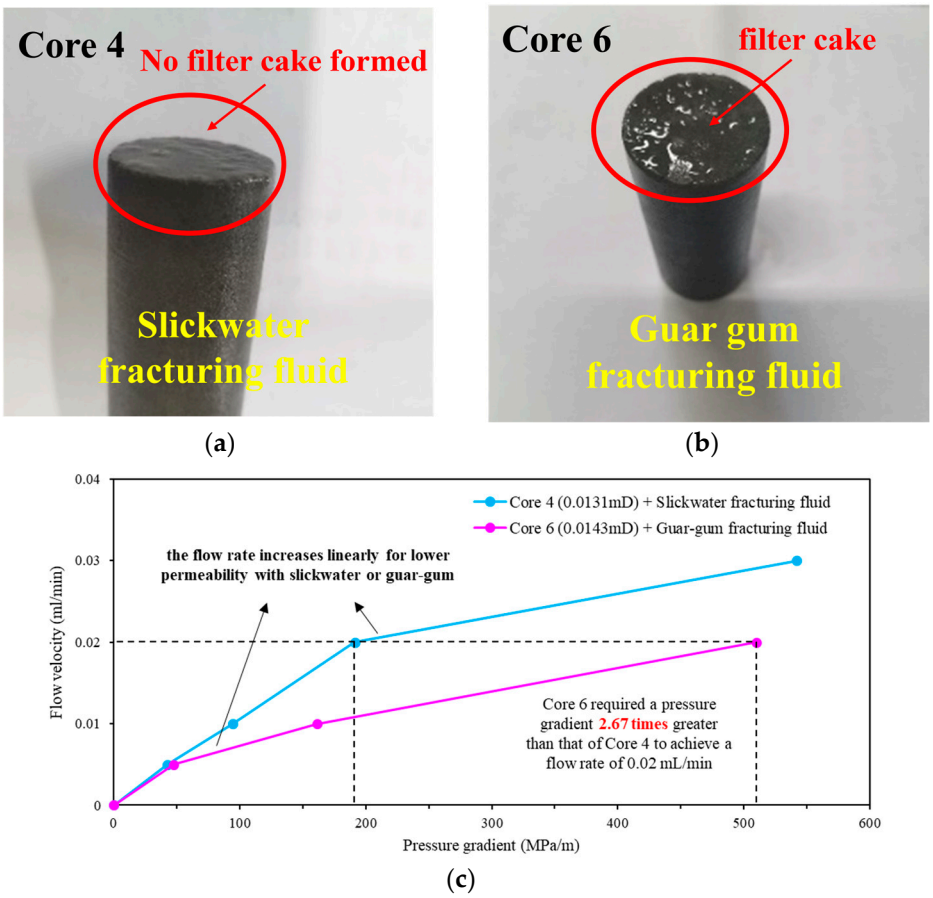

Figure 15. (**a**) Inlet end of core after the application of slickwater fracturing fluid in single-phase percolation mechanism experiment (Core 4); (**b**) inlet end of core after application of the guar gum fracturing fluid in single-phase percolation mechanism experiment (Core 6); (**c**) percolation characteristic curves of Core 4 with the slickwater fracturing fluid and Core 6 with the guar gum fracturing fluid.

Figure 15c displays the percolation characteristic curves of Core 4 treated with slickwater fracturing fluid and Core 6 treated with guar gum fracturing fluid. Although Core 4 (liquid-measured permeability of 0.0131 mD) and Core 6 (liquid-measured permeability of 0.0143 mD) have similar permeabilities, Core 6 exhibits a more pronounced nonlinearity, with a pressure gradient at the same flow rate that is 2.67 times higher than that of Core 4. This greater nonlinearity suggests that the larger macromolecules in the guar gum fluid caused significant blockage, restricting fluid flow and leading to the formation of a filter cake layer. The inability of these larger particles to navigate the tight pore structure intensifies flow resistance, causing a more substantial reduction in permeability and contributing to the nonlinear curve [42].

To further understand the nonlinear behavior of the percolation curves, we compared the results from cores with similar permeabilities in the core damage experiment in Section 3.2. Core 9, injected with slickwater fracturing fluid, exhibited a liquid-measured permeability of 0.0137 mD and a damage percentage of 24.90%. In contrast, Core 14, treated with guar gum fracturing fluid, had a liquid-measured permeability of 0.0106 mD and a damage percentage of 51.89%, which is 2.08 times higher than that of Core 4. This comparison provides critical insights into the performance of the two fracturing fluids. Core 4, treated with slickwater, showed no filter cake formation, whereas Core 6, treated with guar gum, developed a filter cake layer. This layer increases blockage and resistance to fluid flow, as evidenced by the more pronounced nonlinearity observed in the percolation curves for Core 6.

The comparative analysis between slickwater and guar gum fracturing fluids underscores the importance of selecting the appropriate fluid type for tight reservoirs. In practical field applications, operators should consider transitioning to slickwater formulations, especially in formations where permeability is low and the risk of blockage is high.

4.2. Effect of HE-BIO Concentration on Oil Recovery and Field Implications

In Section 3.4, Figures 13 and 14 display a clear trend of increasing oil recovery with higher concentrations of HE-BIO. This enhancement can be attributed to several mechanisms activated by HE-BIO under laboratory conditions:

(1) Enhanced microbial activity. As HE-BIO concentration increases, the population of Bacillus velezensis also grows, thriving in the controlled laboratory environment. These microbes produce CO_2 and biosurfactants that are essential for oil recovery. Higher microbial concentrations lead to greater CO_2 production, which lowers oil viscosity and enhances oil mobility, thus boosting recovery rates.

(2) Increased production of biosurfactants. HE-BIO contains lipopeptide biosurfactants that significantly reduce oil–water interfacial tension and modify the wettability of rock surfaces. With higher HE-BIO concentrations, more biosurfactants are involved, which promotes more effective oil displacement by reducing the adhesion of oil droplets to the rock surfaces. This improved wettability facilitates the flow of oil out of the rock matrix, further enhancing recovery.

(3) Optimized pore utilization. Due to its nanoscale dimensions, HE-BIO can penetrate the small pore spaces in the rock matrix more effectively. As HE-BIO concentration increases, the fluid is better able to navigate the reservoir's microstructures, ensuring more uniform and comprehensive oil displacement throughout the pore network.

However, as HE-BIO concentration continues to rise, the rate of recovery improvement begins to diminish. This trend can be attributed to the reduction in oil–water interfacial tension that occurs with increasing biosurfactant concentration. Although this reduction initially enhances oil recovery, it eventually reaches a point where further improvements become marginal. From a laboratory perspective, this critical concentration is observed to be around 2.0%

The laboratory conditions in this study were carefully designed to closely replicate real reservoir environments, including samples, temperature, and pressure [43], making the findings applicable to field settings. Both the slickwater fracturing fluid and HE-BIO are anticipated to perform similarly in actual reservoirs, providing a reliable approach to enhancing oil recovery.

4.3. Comparison with Conventional Hydraulic Fracturing

In developing tight reservoirs, the coordinated mechanism of HE-BIO and slickwater has been found to significantly increase production. Figure 16 compares the enhanced integrated fracturing process to a conventional hydraulic fracturing process.

Based on the synergistic effect of slickwater fracturing fluid and HE-BIO, the integrated fracturing oil displacement can be divided into several stages:

Phase 1: Fracture formation. Slickwater fracturing fluids, known for their high injection rates (typically 10–20 m^3/min) [44], tend to create longer and more complex fracture networks compared to other fluids. These fractures provide a larger contact area between the reservoir matrix and the fracturing fluid, allowing for more efficient fluid–rock interaction. In particular, the network of fractures enhances the penetration of both the slickwater fracturing fluid and the HE-BIO, improving the effectiveness of the treatment at both macro and micro scales.

Phase 2: Reservoir modification. The HE-BIO modifies the reservoir properties by leveraging the metabolic processes of Bacillus velezensis. Under reservoir conditions, these bacteria produce CO_2, which emulsifies crude oil, reducing its viscosity and improving oil mobility. Additionally, the biological surfactants produced, such as lipopeptides, signifi-

cantly reduce oil–water interfacial tension, altering the wettability of the reservoir's porous media and promoting more efficient oil displacement.

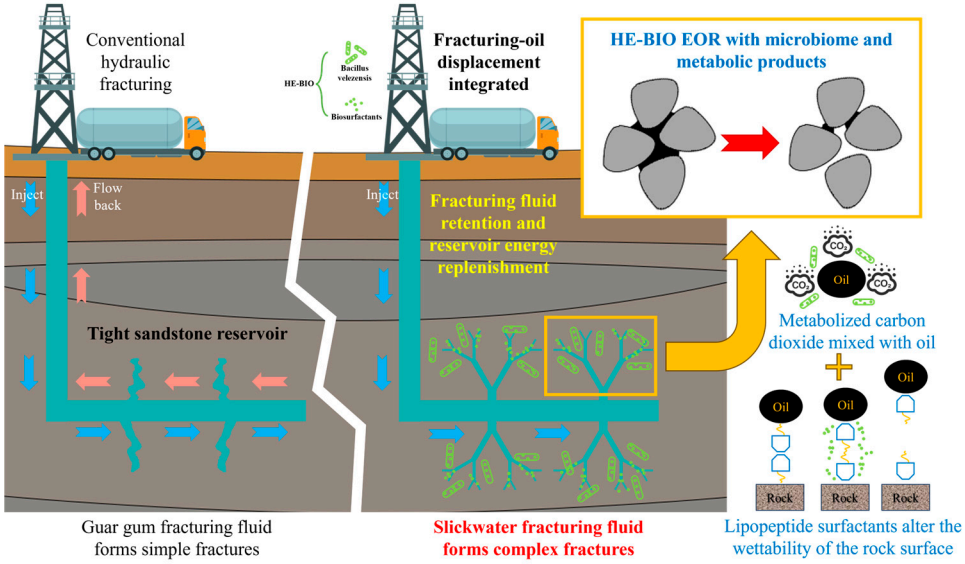

Figure 16. The coordinated mechanism of HE-BIO and slickwater fracturing fluid.

Phase 3: Oil–water displacement. Since the slickwater fracturing fluid causes less damage to the matrix, the fluid can be used without flowing back after fracturing. The significant injection volume of slickwater increases reservoir pressure, facilitating the flow of crude oil from matrix micropores to fractures. Additionally, the intricate network of fractures ensures multiple pathways for fluid displacement, accelerating the process of oil recovery.

The coordinated mechanism of slickwater fracturing fluid and HE-BIO achieves an efficient production increase in tight oil reservoir development by optimizing the fracture network, modifying the reservoir properties, enhancing the seepage-absorption effect, and supplementing the reservoir energy. This innovative fracturing technology provides a new method for the economic development of low-permeability and tight reservoirs.

By examining the micro-percolation characteristics and oil recovery rates, this study offers valuable insights into the potential of integrated fracturing fluid. The conclusions drawn from this research could serve as a foundation for optimizing field applications, as summarized in the final section.

5. Conclusions

This study demonstrates that the slickwater fracturing fluid combined with HE-BIO presents an effective solution for enhancing oil recovery in tight sandstone reservoirs, particularly in the Ordos Basin, where low permeability and complex geological structures pose significant development challenges. Key findings from the experiments conducted include the following:

(1) The slickwater (0.1% JHFR-2 + 0.2% JHFD-2) exhibited improved fluidity and reduced damage to the reservoir matrix compared to traditional guar gum fracturing fluids. Specifically, the matrix damage was reduced by an average of 28.8%, compared to 51.5% with guar gum fluids, underscoring the suitability of the integrated fracturing fluid for tight reservoirs.

(2) The addition of HE-BIO to the slickwater fracturing fluid successfully reduced interfacial tension to less than 7.038 mN/m, a marked improvement over formation water alone, which had an interfacial tension of 22.079 mN/m. This demonstrates the efficacy of HE-BIO as a surfactant in lowering the interfacial tension, thereby enhancing oil displacement capabilities.

(3) A 2.0% concentration of HE-BIO was identified as the optimal balance between recovery performance and cost-effectiveness. While a 2.5% concentration yielded a slightly higher recovery rate of 53.44%, the 2.0% concentration achieved a recovery rate of 53.21% at a reduced cost, making it the most economical choice for maximizing oil recovery (improved by 14%).

For future research, field-scale trials of this HE-BIO-enhanced slickwater fluid are recommended to assess its effectiveness and stability in diverse reservoir conditions. Additionally, exploring the long-term impacts of biosurfactants on reservoir properties, along with potential refinements in fluid composition for environmental compatibility, will be essential. Investigating the synergistic effects of biosurfactants with other additives could further enhance this technology's adaptability to other tight and ultra-low-permeability formations worldwide.

Author Contributions: Conceptualization, P.F. and Y.L.; methodology, P.F.; validation, Y.L., Z.L. and H.G.; formal analysis, H.G.; investigation, P.L.; resources, P.L.; data curation, P.F.; writing—original draft preparation, P.F.; writing—review and editing, Y.L.; visualization, Z.L.; supervision, P.L.; project administration, Z.L.; funding acquisition, Y.L. All authors have read and agreed to the published version of the manuscript.

Funding: This research was funded by the National Major Science and Technology Projects of China (No. 2017ZX05032004-002), the Natural Science Foundation of Beijing Province (No. 3222037), the Shaanxi Province Technology Innovation Guidance Special Plan Project (No. 2023-YD-CGZH-02), and the Major Science and Technology Projects of PetroChina (No. 2020D-5007-0203).

Data Availability Statement: The data presented in this study are available on request from the corresponding author. The data are not publicly available due to licensing agreements.

Conflicts of Interest: Authors Pingtian Fan and Ping Li were employed by the Nanniwan Oil Production Plant, Yanchang Oilfield Co., Ltd. The remaining authors declare that the research was conducted in the absence of any commercial or financial relationships that could be construed as a potential conflict of interest. Furthermore, the funding sponsors had no role in the design of the study; in the collection, analyses, or interpretation of data; in the writing of the manuscript, and in the decision to publish the results.

References

1. Sun, L.; Zou, C.; Jia, A.; Wei, Y.; Zhu, R.; Wu, S.; Guo, Z. Development Characteristics and Orientation of Tight Oil and Gas in China. *Pet. Explor. Dev.* **2019**, *46*, 1073–1087. [CrossRef]
2. Zhao, W.; Hu, S.; Hou, L.; Yang, T.; Li, X.; Guo, B.; Yang, Z. Types and Resource Potential of Continental Shale Oil in China and Its Boundary with Tight Oil. *Pet. Explor. Dev.* **2020**, *47*, 1–11. [CrossRef]
3. Zhang, J.; Gao, M.; Dong, J.; Yu, T.; Ding, K.; Liu, Y. Assessment of Refracturing Potential of Low Permeability Reservoirs Based on Different Development Approaches. *Energies* **2024**, *17*, 2526. [CrossRef]
4. Zhu, R.; Zou, C.; Mao, Z.; Yang, H.; Hui, X.; Wu, S.; Cui, J.; Su, L.; Li, S.; Yang, Z. Characteristics and Distribution of Continental Tight Oil in China. *J. Asian Earth Sci.* **2019**, *178*, 37–51. [CrossRef]
5. Yu, L.; Wang, J.; Wang, C.; Chen, D. Enhanced Tight Oil Recovery by Volume Fracturing in Chang 7 Reservoir: Experimental Study and Field Practice. *Energies* **2019**, *12*, 2419. [CrossRef]
6. Mardashov, D.; Duryagin, V.; Islamov, S. Technology for Improving the Efficiency of Fractured Reservoir Development Using Gel-Forming Compositions. *Energies* **2021**, *14*, 8254. [CrossRef]
7. Guo, T.; Zhang, S.; Qu, Z.; Zhou, T.; Xiao, Y.; Gao, J. Experimental Study of Hydraulic Fracturing for Shale by Stimulated Reservoir Volume. *Fuel* **2014**, *128*, 373–380. [CrossRef]
8. Xu, D.; Chen, S.; Chen, J.; Xue, J.; Yang, H. Study on the Imbibition Damage Mechanisms of Fracturing Fluid for the Whole Fracturing Process in a Tight Sandstone Gas Reservoir. *Energies* **2022**, *15*, 4463. [CrossRef]
9. Jie, Y.; Yang, J.; Zhou, D.; Wang, H.; Zou, Y.; Liu, Y.; Zhang, Y. Study on the Optimal Volume Fracturing Design for Horizontal Wells in Tight Oil Reservoirs. *Sustainability* **2022**, *14*, 15531. [CrossRef]
10. Al-Muntasheri, G.A. A Critical Review of Hydraulic-Fracturing Fluids for Moderate- to Ultralow-Permeability Formations Over the Last Decade. *SPE Prod. Oper.* **2014**, *29*, 243–260. [CrossRef]
11. Yao, E.; Bai, H.; Zhou, F.; Zhang, M.; Wang, J.; Li, F. Performance Evaluation of the Multifunctional Variable-Viscosity Slick Water for Fracturing in Unconventional Reservoirs. *ACS Omega* **2021**, *6*, 20822–20832. [CrossRef] [PubMed]
12. Wang, J.; Zhou, F.; Bai, H.; Li, Y.; Yang, H. A Comprehensive Method to Evaluate the Viscous Slickwater as Fracturing Fluids for Hydraulic Fracturing Applications. *J. Pet. Sci. Eng.* **2020**, *193*, 107359. [CrossRef]

13. Brannon, H.D.; Bell, C.E. Eliminating Slickwater Compromises for Improved Shale Stimulation. In Proceedings of the SPE Annual Technical Conference and Exhibition, Denver, CO, USA, 30 October–2 November 2011; p. SPE-147485-MS. [CrossRef]
14. Palisch, T.T.; Vincent, M.C.; Handren, P.J. Slickwater Fracturing: Food for Thought. *SPE Prod. Oper.* **2010**, *25*, 327–344. [CrossRef]
15. Yang, B.; Zhang, H.; Kang, Y.; You, L.; She, J.; Wang, K.; Chen, Z. In Situ Sequestration of a Hydraulic Fracturing Fluid in Longmaxi Shale Gas Formation in the Sichuan Basin. *Energy Fuels* **2019**, *33*, 6983–6994. [CrossRef]
16. Li, S.; Cai, B.; He, C.; Gao, Y.; Wang, J.; Yan, F.; Liu, Y.; Yu, T.; Zhong, X.; Cheng, N.; et al. Frac Fluid Induced Damage in Tight Sands and Shale Reservoirs. In Proceedings of the SPE International Conference and Exhibition on Formation Damage Control, Lafayette, LA, USA, 23–24 February 2022; p. D022S010R003. [CrossRef]
17. Islamov, S.; Islamov, R.; Shelukhov, G.; Sharifov, A.; Sultanbekov, R.; Ismakov, R.; Agliullin, A.; Ganiev, R. Fluid-Loss Control Technology: From Laboratory to Well Field. *Processes* **2024**, *12*, 114. [CrossRef]
18. Khormali, A. Inhibition of Barium Sulfate Precipitation During Water Injection into Oil Reservoirs Using Various Scale Inhibitors. *Arab. J. Sci. Eng.* **2023**, *48*, 9383–9399. [CrossRef]
19. Yan, J.; Li, Y.; Xie, X.; Slaný, M.; Dong, S.; Wu, Y.; Chen, G. Research of a Novel Fracturing-Production Integral Fluid Based on Cationic Surfactant. *J. Mol. Liq.* **2023**, *369*, 120858. [CrossRef]
20. Cong, S.; Li, J.; Liu, W.; Shi, Y.; Li, Y.; Zheng, K.; Luo, X.; Luo, W. EOR Mechanism of Fracture Oil Displacement Agent for Ultra-Low Permeability Reservoirs. *Energy Rep.* **2023**, *9*, 4893–4904. [CrossRef]
21. Gao, M.-W.; Zhang, M.-S.; Du, H.-Y.; Zhao, M.-W.; Dai, C.-L.; You, Q.; Liu, S.; Jin, Z.-H. A Novel Triple Responsive Smart Fluid for Tight Oil Fracturing-Oil Expulsion Integration. *Pet. Sci.* **2023**, *20*, 982–992. [CrossRef]
22. Zhang, X.; Jia, H.; Wu, G.; Xu, M.; Li, C.; Wei, Z.; Cao, W.; Wang, X.; Lv, K.; Liu, D.; et al. Performance Evaluation and Formation Mechanism of Janus-SiO_2 Nanoparticles Assisted Viscoelastic Surfactant Fracturing Fluids. *J. Mol. Liq.* **2023**, *390*, 123203. [CrossRef]
23. Gao, H.; Li, X.; Li, T.; Cheng, Z.; Wang, C.; Zhu, X.; Han, B.; Luo, K.; Wang, W.; Ren, X. Characteristics of Oil Production by Fracturing Fluid Additive-Assisted Displacement in Tight Oil Reservoirs. *Energy Fuels* **2024**, *38*, 17541–17553. [CrossRef]
24. Zhang, Y.; You, Q.; Fu, Y.; Zhao, M.; Fan, H.; Liu, Y.; Dai, C. Investigation on Interfacial/Surface Properties of Bio-Based Surfactant N-Aliphatic Amide-N,N-Diethoxypropylsulfonate Sodium as an Oil Displacement Agent Regenerated from Waste Cooking Oil. *J. Mol. Liq.* **2016**, *223*, 68–74. [CrossRef]
25. Wang, B.; Wang, S.; Yan, H.; Bai, Y.; She, Y.; Zhang, F. Synthesis and Enhanced Oil Recovery Potential of the Bio-Nano-Oil Displacement System. *ACS Omega* **2023**, *8*, 16139–16150. [CrossRef] [PubMed]
26. Feng, Q.; Zhou, J.; Li, S.; Chen, X.; Sun, Y.; Zhang, X.; Gao, P.; Zhang, F.; She, Y. Research on Characterization Technology and Field Test of Biological Nano-Oil Displacement in Offshore Medium- and Low-Permeability Reservoirs. *ACS Omega* **2022**, *7*, 35087–35100. [CrossRef]
27. Al-Ghailani, T.; Al-Wahaibi, Y.M.; Joshi, S.J.; Al-Bahry, S.N.; Elshafie, A.E.; Al-Bemani, A.S. Application of a New Bio-ASP for Enhancement of Oil Recovery: Mechanism Study and Core Displacement Test. *Fuel* **2021**, *287*, 119432. [CrossRef]
28. Althalb, H.A.; Elmusrati, I.M.; Banat, I.M. A Novel Approach to Enhance Crude Oil Recovery Ratio Using Selected Bacterial Species. *Appl. Sci.* **2021**, *11*, 10492. [CrossRef]
29. Han, H.; Zhu, W.; Song, Z.; Yue, M. Mechanisms of Oil Displacement by Geobacillus Stearothermophilus Producing Bio-Emulsifier for MEOR. *Pet. Sci. Technol.* **2017**, *35*, 1791–1798. [CrossRef]
30. Wu, B.; Xiu, J.; Yu, L.; Huang, L.; Yi, L.; Ma, Y. Biosurfactant production by Bacillus subtilis SL and its potential for enhanced oil recovery in low permeability reservoirs. *Sci. Rep.* **2022**, *12*, 7785. [CrossRef]
31. Zhao, W.; Hou, G. Fracture prediction in the tight-oil reservoirs of the Triassic Yanchang Formation in the Ordos Basin, northern China. *Pet. Sci.* **2017**, *14*, 1–23. [CrossRef]
32. Li, Z.; Qu, X.; Liu, W.; Lei, Q.; Sun, H.; He, Y. Development Modes of Triassic Yanchang Formation Chang 7 Member Tight Oil in Ordos Basin, NW China. *Pet. Explor. Dev.* **2015**, *42*, 241–246. [CrossRef]
33. He, S.; Huang, T.; Bai, X.; Ren, J.; Meng, K.; Yu, H. Dramatically Enhancing Oil Recovery via High-Efficient Re-Fracturing Horizontal Wells in Ultra-Low Permeability Reservoirs: A Case Study in HQ Oilfield, Ordos Basin, China. *Processes* **2024**, *12*, 338. [CrossRef]
34. Yaich, E.; Williams, S.; Bowser, A.; Goddard, P.; Diaz De Souza, O.C.; Foster, R.A. A Case Study: The Impact of Soaking on Well Performance in the Marcellus. In Proceedings of the 3rd Unconventional Resources Technology Conference, San Antonio, TX, USA, 20–22 July 2015. [CrossRef]
35. You, L.; Zhang, N.; Kang, Y.; Xu, J.; Cheng, Q.; Zhou, Y. Zero Flowback Rate of Hydraulic Fracturing Fluid in Shale Gas Reservoirs: Concept, Feasibility, and Significance. *Energy Fuels* **2021**, *35*, 5671–5682. [CrossRef]
36. Wang, J.; Zhou, F.; Bai, H.; Wei, D.; Ma, J.; Yang, P.; Zhang, F.; Yuan, L. A New Approach to Study the Friction-Reduction Characteristics of Viscous/Conventional Slickwater in Simulated Pipelines and Fractures. *J. Nat. Gas Sci. Eng.* **2020**, *83*, 103620. [CrossRef]
37. Bai, H.; Zhou, F.; Zhang, M.; Gao, X.; Xu, H.; Yao, E.; Wang, J.; Li, Y. Optimization and Friction Reduction Study of a New Type of Viscoelastic Slickwater System. *J. Mol. Liq.* **2021**, *344*, 117876. [CrossRef]
38. Shi, Y.; Yu, W.; Zhou, D.; Ding, F.; Shu, W.; Zhang, Y.; Ju, Y.; Lei, Z. Research on the Performance of New Weighted Slippery Water Fracturing Fluid System. *Open J. Appl. Sci.* **2024**, *14*, 2101–2111. [CrossRef]

39. Fan, Y.; Yu, W.; Shu, W.; Zhang, Y.; Ju, Y.; Fan, P. Synthesis and performance evaluation of low-damage variable viscosity integrated drag reducer. *J. Appl. Polym. Sci.* **2024**, *141*, e55925. [CrossRef]
40. Zhang, Y.; Wang, J.; Liu, Y.; Yu, T.; He, C.; Chen, S. Halotolerant Bacillus Velezensis Sustainably Enhanced Oil Recovery of Low Permeability Oil Reservoirs by Producing Biosurfactant and Modulating the Oil Microbiome. *Chem. Eng. J.* **2023**, *453*, 139912. [CrossRef]
41. McClements, D.J.; Gumus, C.E. Natural Emulsifiers—Biosurfactants, Phospholipids, Biopolymers, and Colloidal Particles: Molecular and Physicochemical Basis of Functional Performance. *Adv. Colloid Interface Sci.* **2016**, *234*, 3–26. [CrossRef]
42. Wang, J.; Huang, Y.; Zhang, Y.; Zhou, F.; Yao, E.; Wang, R. Study of Fracturing Fluid on Gel Breaking Performance and Damage to Fracture Conductivity. *J. Pet. Sci. Eng.* **2020**, *193*, 107443. [CrossRef]
43. Fan, P.; Liu, Y.; Li, P.; Guo, Y.; Yu, W.; Li, B. Reservoir Sensitivity Analysis of Tight Sandstone and Its Controlling Factors: A Case Study from Chang 4+5 to Chang 6 Reservoirs in N 212 Well Block of Nanniwan Oilfield, Ordos Basin. *Geofluids* **2023**, *2023*, 8878837. [CrossRef]
44. Detournay, E. Slickwater Hydraulic Fracturing of Shales. *J. Fluid Mech.* **2020**, *886*, F1. [CrossRef]